http://dx.doi.org/10.21611/qirt.1992.003

Improving the accuracy of inferred temperatures in small spot size experiments

by J. PEARCE(*), M. SCHULZE (*) and Z. RYU (**)

(*) *Biomedical Engineering Program, The University of Texas at Austin, Austin Texas, USA.*

(**) *Goldstar Co. Ltd. Seoul, Korea.*

Abstract

Accurate inference of surface temperature distribution in transient thermal images requires the reduction of detector noise effects, correction for small features in a relatively large Instantaneous Field Of View (IFOV) imager, and correction for thermal gradients along the optical axis. We have investigated non linear smoothing operators, specifically the median filter and linear combinations of non linear morphologic operators. Both types are effective but the one-dimensional median filter is both most accurate, simplest and fastest to implement and use. The underestimated caused by IFOV problems is best corrected by Wiener filter de-convolution, in our view. Finally, optical axis thermal gradients can require significant correction factors to be applied to the measured emittance in order to estimate maximum surface temperature.

Nomenclature

α	Space decay constant for non uniform subsurface temperature (m^{-1})
E	Emissive fluence rate of surface (W/m^2)
f	Two-dimensional image function
F	Frequency domain representation (Fourier transform) of f
g	Two-dimensional image function
G	Frequency domain representation of g
h	Point spread function of an imaging device (two-dimensional)
H	Optical transfer function (Fourier transform of h)
M	Median filter operator
μ	Optical attenuation coefficient in medium for imaging wavelengths
n	Window size parameter for sliding window filter
N	Frequency domain representation of imager noise process
P	Volumetric radiative power density of participating medium (W/m^3)
σ	Gaussian distribution parameter
U	Estimate of uncorrupted (noise-free) image, frequency domain
w	Window width for sliding window filter
W	Wiener filter transfer function (frequency domain)
z	Optical axis for imaging system (m)

1. Introduction

Temperatures inferred from measurements of surface emittance are subject to errors due to: emissivity variations; surface reflectance; the non linear relationship between emittance and surface temperature for band-limited imagers; and optical pathway attenuation in mirrors and lenses. Strategies for dealing with these sources are well documented. Other error sources include: the thermal noise source in the detector, primarily recombination-generation noise, an impulse-like process; finite

http://dx.doi.org/10.21611/qirt.1992.003

detector field of view including slew rate limitations in a flying spot device; and temperature gradients along the optical axis.

2. Strategies for addressing the problems

2.1. Noise reduction filters

The most attractive method for reducing detector noise effects is signal averaging. This approach is effective when the thermal scene is stationary. For fast transient thermal images, such as those of laser spots on tissue, frame averaging cannot be used. In transient scenes the detector noise must be reduced on single images with very little *a priori* information.

2.1.1. Median filters

14 The most powerful linear operator is the Wiener filter (§ 2.2), which depends on accurate measurement of the imager point spread function and complete statistics of the noise process for best results. The Wiener filter is optimal in the mean square sense, which may not always be the most desirable criterion. Also, it is computationally intensive, performs very poorly near the edges of the image, and, like all linear operators, smears edges and other fine details.

We have found that non linear order statistic filters, in particular the median filter, are well suited to thermal image noise reduction. The median filter is implemented by replacing the image value of the pixel in the center of a window by the value in the center of the ranked sequence. The median filter is non linear because, in general, superposition does not apply:

$$M\left\{a\,\mathbf{f}(x,y) + b\,\mathbf{g}(x,y)\right\} \neq a\,M\left\{\mathbf{f}(x,y)\right\} + b\,M\left\{\mathbf{g}(x,y)\right\} \qquad (1)$$

where bold face characters represent random processes and a and b are arbitrary constants. For two random processes which have symmetrical simply-connected probability density functions (PDF), the process median equals the process mean and the median filter will, in some sense, mimic the output of a mean filter. The median filter is simultaneously noise-reducing and edge-preserving, thus possessing both high-pass and low-pass characteristics due to its non linear nature. The median filter eliminates impulse noise (without changing data values) and does not change monotonic sequences (edges).

In a flying spot scanner thermal imaging device, the detector noise process is equivalent to a one-dimensional spatial noise process due to the raster scan. We estimated the probability density function for an Inframetrics Model 525 scanner using 1792 pixels from two black bodies, as shown in *figure 1*. The histograms are similar to gaussian PDFs with $\sigma \cong 0.21$ °C. The calibrated power spectral density for our scanner is shown in *figure 2* . A barely-discernable inverse of frequency component dominates below about 300 kHz with approximately white noise at higher frequencies

The median filter works against the detector noise process to reduce the minimum resolvable temperature difference (MRTD) nearly as well as the Wiener filter. The window width ($w = 2n + 1$) is the only parameter which can be adjusted when using the median filter. The value of n defines an impulse for the filter: an impulse is n or

http://dx.doi.org/10.21611/qirt.1992.003

less points different in value from the surrounding sequences. An unfiltered bar pattern image (bars 11 pixels wide) with an MRTD of 0.42 °C improves to 0.18 °C under median filtering ($w = 5$), and to 0.12 °C for a Wiener filter, cf *figure 3*. As the bar pattern spatial frequency increases, the edge smearing effect of the linear filter results in an increase in the MRTD while the median filtered result is unaffected until the bar width decreases to n+1 or less pixels.

Of interest is the fact that the median filter is unbiased but does introduce edge-jitter, however due to the ranking nature of the processor. The thermal camera creates the raster with an oscillating horizontal mirror which has horizontal phase errors due to mirror position uncertainty and detector slew-rate limitations. We have found that applying the one-dimensional median filter horizontally with a 5-wide window ($n = 2$) followed by a vertical 3-wide one-dimensional triangular window reduces detector noise and edge jitter with the best overall accuracy — we call this strategy the Ryu window for thermal images.

2.1.2. Linear combinations of morphologic operators

Morphologic operators are based on heuristic rules applied to a *structuring element* (a window of arbitrary shape). The operations are two: *erosion* which enlarges dark areas; and *dilation* which enlarges lighter areas. An *open* operation is an erosion followed by a dilation, and a *close* operation is a dilation followed by an erosion. The next level of cascade, either a *close-open* (CO) or an *open-close* (OC) can be used to reduce noise effects. Both CO and OC operations introduce bias in the PDF; the CO operator biases the PDF toward higher temperatures and the OC operation toward lower temperatures. Neither is acceptable in quantitative thermal imaging.

Linear combinations of the cascaded morphological operators will virtually eliminate the bias. We call the linear combination filter a LOCO operator. The linear combination of non linear operators reduces the bias to acceptable levels; however, in terms of overall accuracy the main disadvantage is that they round off the top of a peaked temperature feature (such as a gaussian shaped thermal spot) more than the Ryu window described above.

2.2. Small spot compensation

The thermal detector instantaneous field of view (IFOV) and slew rate limit the accuracy of small spot image temperatures. The Wiener filter is effective in de-convolving errors due to spot size; thus providing more accurate estimates of center peak center temperature in small spot size images. The well-known Wiener filter is given by:

$$\mathbf{W}(u, v) = \frac{H^*(u, v)}{|H(u, v)|^2 + \dfrac{\mathbf{N}(u, v)}{\mathbf{F}(u, v)}} \cong \frac{H^*(u, v)}{|H(u, v)|^2 + \dfrac{\text{Noise}}{\text{Signal}}} \tag{2}$$

where W is the filter function, H is the optical transfer function (OTF) for the imager with complex conjugate H*, **N** is the noise process, **F** the image and u and v are spatial frequencies. Usually **N** and **F** are not known so the ratio is replaced by the inverse of the signal to noise ratio. The estimate of the original image, **U**, is obtained from the convolution of W with the corrupted image **G** where we have assumed additive noise:

http://dx.doi.org/10.21611/qirt.1992.003

$$\boldsymbol{U}(u, v) = W(u, v)\,\boldsymbol{G}(u, v) = W(u, v)\left\{\boldsymbol{F}(u, v)\,H(u, v) + \boldsymbol{N}(u, v)\right\} \qquad (3)$$

The point spread function for the Inframetrics detector and associated optics is approximately a gaussian function, as shown in *figure 4.*

2.3. Temperature gradients along the optical axis

When significant gradients exist on the optical axis, often the case for laser spots, the surface temperature may be significantly under estimated. If the depth of penetration of the laser is less than the viewing depth of the camera then the total surface emittance will be less than if the temperature was constant. Very high absorption coefficient lasers — Er:YAG, Ho:YAG, excimer — which have optical depths on same the order, or much less than, the camera generate significantly less surface emittance than they would if the temperature were constant over the viewing depth. The black body surface emittance, E (W/m^2), is the sum of volumetric radiation, P (W/m^3), which reaches the surface. If P is a constant then:

$$E(T) = \int_0^{\infty} P(T)\, e^{-\mu z}\, dz = \frac{P(T)}{\mu} \qquad (4)$$

A black surface with $T(z) = T(0)\, e^{-\alpha z}$ viewed with a camera whose attenuation coefficient is μ would need a correction factor applied to the measured emittance of $(\alpha + \mu)/\mu$. For a tissue surface viewed with an 8 to 12 µm camera, the correction coefficients range from 1.0001 for the Nd:YAG laser to 13.6 for the XeCl laser assuming adiabatic (i.e. very short pulse) heating. Note that the correction coefficient is applied to the surface power. A summary of calculated correction factors is given in *table I.*

3. Conclusions

Digital filtering methods can be used to reduce uncertainty in thermal images of transient small spot size patterns. Non linear filtering against detector noise has the advantage that impulsive noise can be eliminated without degrading image edges and other fine features; however, bias may be introduced by asymmetrical operators. When the thermal feature is not large compared to the IFOV the center temperature will be significantly under estimated. Wiener filter de-convolution provides the most effective compensation strategy. Negative thermal gradients within the imager viewing depth give an under-estimate of surface temperature — correction factors are often quite large for ordinary laser spots on tissue, as an example.

4. Acknowledgement

This work was partially supported by the National Science Foundation (US), under grant number BCS 845-1123.

http://dx.doi.org/10.21611/qirt.1992.003

TABLE I

Calculated correction factors specific for the 8 to 12 μm imaging band assuming laser impingement on tissue.

Laser Type	Wavelength (μm)	Optical Depth (μm)	Correction Factor
CO_2	10.6	12.6	(*2.0)
Er:YAG	2.94	1.0	13.6
Nd:YAG	1.06	11 111	1.001
Ar	0.514	909	1.01
Xe-Cl	0.308	100	1.12
Kr-F	0.248	50	1.25
Ar-F	0.193	<1	>13.6

* Note: the 8 to 12 μm camera cannot be used while the CO_2 laser is on since reflected laser light will obscure surface emittance.

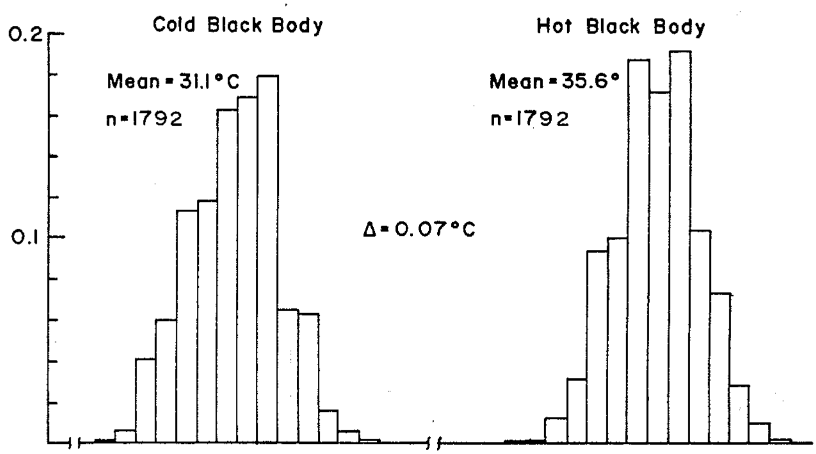

Fig. 1. - Measured noise process histogram on two black body surfaces with 1792 points selected from the constant temperature region.

http://dx.doi.org/10.21611/qirt.1992.003

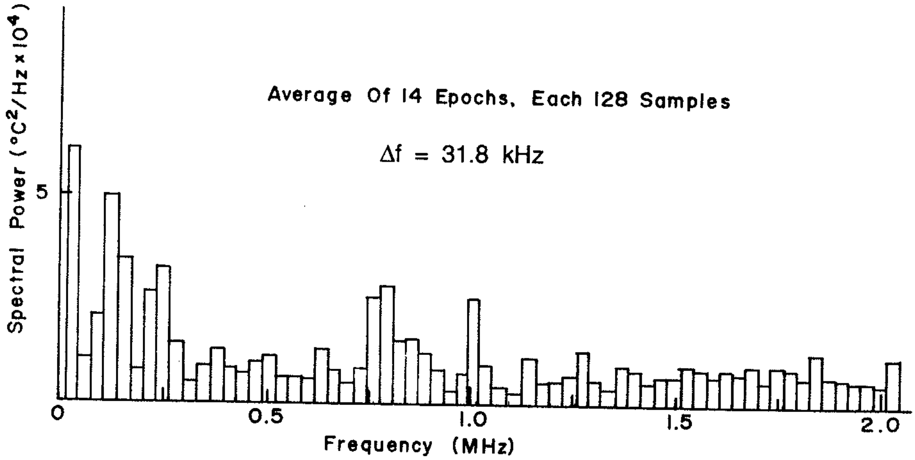

Fig. 2. - Calibrated power spectral density cf fig. 1.

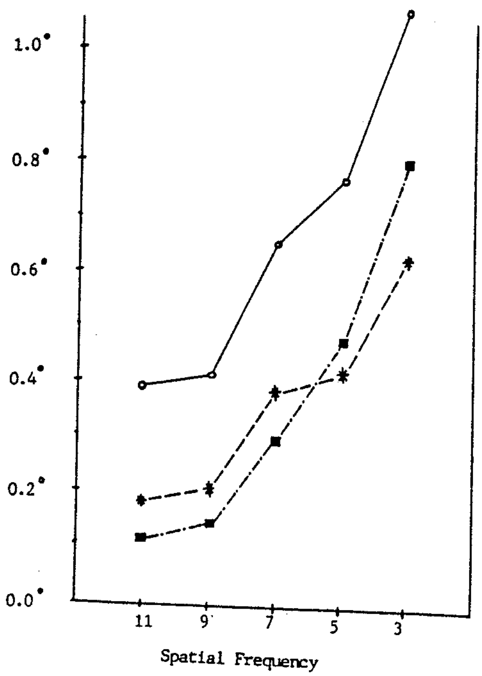

Fig. 3. - Minimum resolvable temperature difference (MRTD) for unfiltered (o), median filtered (*), and Wiener filtered (squares) bar pattern. The window width was maintained at 5 as the bar width decreased from 11 to 3 pixels.

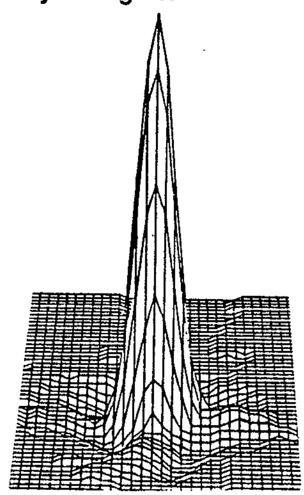

Fig. 4. - Point spread function from measurements of the edge spread function at 5° intervals over 0 to 180°. The camera was set for maximum field of view. Horizontal direction is parallel with the page while the vertical direction is into the page.